Check for updates

Impact of Defects on Electronic Properties of Heterostructures Constructed From Monolayers of Transition Metal Dichalcogenides

Victor L. Shaposhnikov, Anna V. Krivosheeva, and Victor E. Borisenko*

Electronic properties of heterostructures composed of two single molecular layers (monolayers) of MoS_2, WS_2, WSe_2, and $MoSe_2$ are ab initio simulated with an emphasis to the stacking peculiarities and an influence of point defects in their lattices. $MoS_2/MoSe_2$, MoS_2/WS_2, WS_2/WSe_2, and $MoSe_2/WSe_2$ heterostructures with the monolayers shifted like in the bulk material have been found to behave like semiconductors with the energy gaps of 0.88, 1.25, 1.06, and 1.07 eV, respectively. Such heterostructures possess indirect gaps in contrast to individual monolayers, while direct-gap character is preserved in two layer stacking variants in WS_2/WSe_2 heterostructures and in $MoS_2/MoSe_2$ heterostructure with mirror stacking of the monolayers. Vacancies and Te atoms substituting other chalcogen atoms reduce the band gaps. The calculated orbital compositions of first direct band gap transitions in the defect-free heterostructures and those with the point defects have demonstrated *d*-electrons of Mo or W atoms to be mainly involved in the transitions.

1. Introduction

Engineering of new electronic devices with an improved performance needs new materials and their based heterostructures. Two-dimensional crystals of semiconducting transition metal dichalcogenides (TMDs) like MoS_2, $MoSe_2$, $MoTe_2$, WS_2, and WSe_2 have been recently shown to be very promising for that.[1–7] They can be fabricated with different numbers of molecular layers down to a thickness of one monolayer. That allows fabrication of nanoscaled low-power field-effect transistors,[1] logic circuits,[2] and phototransistors.[3–7] Recently, single-layer materials got great interest because of their optical properties and prospects in nanophotonics.[8] While bulk MoS_2, WS_2, WSe_2, and $MoSe_2$ are indirect-gap semiconductors,[9,10] first direct transitions become dominating in crystalline monolayers of some TMDs.[11] That makes them applicable in new optoelectronic devices and sensors. However, two and more monolayers of the same TMD demonstrate an indirect-gap behavior.[12]

Experimentally observed indirect energy gap (E_g) in bulk MoS_2 ranges from 1.23 to 1.29 eV and E_g in WS_2 is of about 1.35 eV[9,13] while monolayers of MoS_2 and WS_2 have direct gaps of about 1.8 eV[11,14] and 2.4 eV,[15] respectively. Theoretical calculations give gaps of 0.90–1.52 eV (indirect gap) for the bulk of MoS_2 and 1.72–1.86 eV (direct gap) in a MoS_2 monolayer, respectively.[16–20] For WS_2 the gaps are 1.63 eV in the bulk material and 2.53 eV in one monolayer.[21]

Combination of the layers of different TMDs gives a possibility to obtain a direct-gap hybrid two-dimensional crystal.[12,22] Such structures can be fabricated by means of a layering technique from already formed monomolecular layers or by their layer-by-layer chemical vapor deposition.[22]

In order to establish peculiarities of fundamental electronic properties of two-dimensional heterostructures made of MoS_2, WS_2, WSe_2, and $MoSe_2$ monolayers, we have ab initio calculated electronic energy band structures of an extended combination of the materials: $MoS_2/MoSe_2$, MoS_2/WS_2, WS_2/WSe_2, and $MoSe_2/WSe_2$. An impact of the stacking arrangement as well as vacancies and substitutional Te atoms were analyzed.

2. Computational Details

Fundamental electronic properties of the heterostructures including electronic energy bands and densities of states (DOS) were calculated using the PAW-LDA approximation[23] within the density functional theory (DFT) realized in the VASP code.[24] We analyzed freestanding heterostructures composed of one monolayer of each material, namely $MoS_2/MoSe_2$, MoS_2/WS_2, WS_2/WSe_2, and $MoSe_2/WSe_2$. We considered 2H phase with the space group $P6_3/mmc$ as the most stable polymorphic modification for this class of hexagonal layered two-dimensional crystals.[25]

The general view of the modeled structures is shown in **Figure 1**. The stacking monolayers were arranged in two

Dr. V. L. Shaposhnikov, Dr. A. V. Krivosheeva, Prof. V. E. Borisenko
Belarusian State University of Informatics and Radioelectronics
P. Browka 6, 220013 Minsk, Belarus
E-mail: victor.shaposhnikov@gmail.com

Prof. V. E. Borisenko
National Research Nuclear University MEPhI (Moscow Engineering Physics Institute)
Kashirskoe shosse 31, 115409 Moscow, Russia

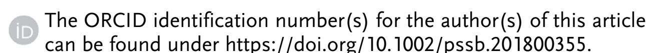
The ORCID identification number(s) for the author(s) of this article can be found under https://doi.org/10.1002/pssb.201800355.

DOI: 10.1002/pssb.201800355

© 2019 WILEY-VCH Verlag GmbH & Co. KGaA, Weinheim

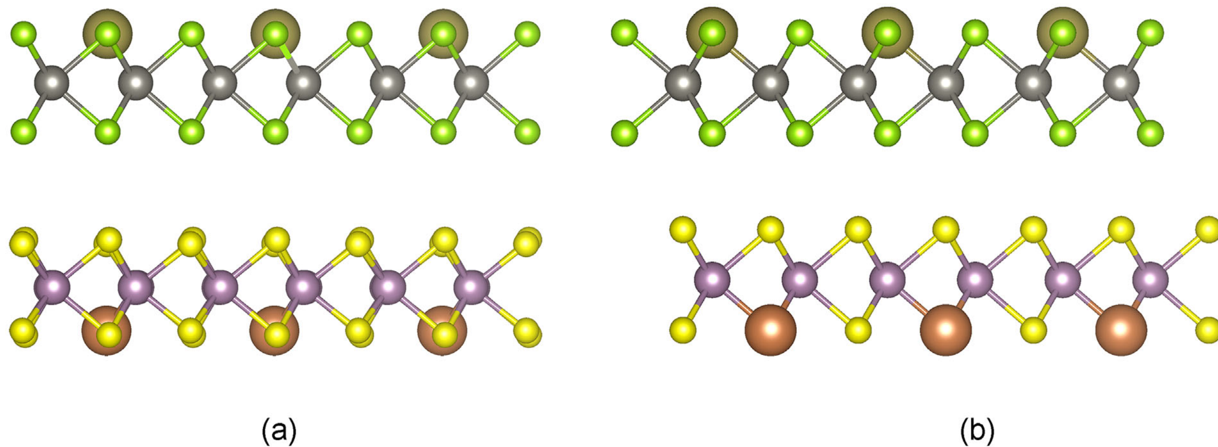

Figure 1. Side view of heterostructures with a mirror arrangement of monolayers (a) and arrangement of the monolayers with a shift typical for the bulk material (b). Dark small balls represent metal atoms, light small balls stand for chalcogen atoms, big balls represent atoms of impurity or vacancies.

possible ways: atoms of the upper layer were located above the atoms of the lower layer in accordance with the mirror symmetry, or the layers were shifted relative to each other in a manner analogous to that in the bulk material. An effect of point defects was analyzed for the case of vacancies or Te atoms in the positions of S or Se atoms.

The translational cell for all structures had 2×2 size and included 8 metal atoms and 16 chalcogen ones. The arrangement of the atoms corresponded to the mentioned above hexagonal structure. One vacancy or one impurity atom was put in one layer. The thickness of the vacuum spacer separating the monolayers was chosen to be 15 Å.

Atomic relaxation via minimization of the total energy of the heterostructures was performed by calculation of Hellmann–Feynman forces and the stress tensor. It was stopped when the forces acting on atoms became less than 0.01 eV $Å^{-1}$. The energy cutoff was fixed at 380 eV. The $9 \times 9 \times 2$ grid of Γ-centered points was used. For representation of the electronic energy band structure 30 k-points were chosen for each segment along high-symmetry directions of the hexagonal Brillouin zone. The van der Waals interaction between the monolayers was treated via the correction proposed by J. Klimeš,[26] known as optB86b-vdW optimized exchange functional and implemented in the VASP code. It provides the structural parameters to be very close to experimental ones. The distance between the monolayers before the relaxation corresponded to the interlayer distance in the bulk material. 4*p*- (5*p*-) electronic states of Mo (W) were considered as valence states. A similar approach has been already successfully tested in the calculations for individual layers of MoS_2, $MoSe_2$, WS_2, and WSe_2.[16,17,27]

It should be noted here that calculations within the DFT approaches without using the electronic self-energy corrections usually underestimate band gaps with respect to the experimental ones. The value of such underestimation depends on the shift of eigenvalues in the energy range analyzed due to the so-called correlation effects. Nevertheless, we have previously obtained a good agreement between experimental data and our theoretical findings for TMDs employing the fact that the corresponding eigenfunctions at the extrema points of the band structure are mainly composed of *d*-electron states of the metal atoms.[16,17] So, they undergo an almost equal shift. Properties of TMDs are strongly influenced by excitonic effects, so the fundamental energy gap of low-dimensional compounds cannot be directly obtained from optical experiments because their optical gaps are smaller than real gaps by the exciton binding energy.[19] Nevertheless, the experimental data on the photoluminescence of MoS_2 layers agree with the theoretical prediction of conversion from indirect to direct-gap semiconductor upon moving from bulk to one monolayer.[14] Moreover, the structural parameters obtained taking into account the van der Waals interaction are much closer to the experimental values than the results obtained within common DFT approaches without considering this interaction.[21] Thus, the method we used can be applicable for qualitative analysis and determination of gap modifications under various conditions.

3. Results and Discussion

The interatomic distances calculated after the lattice relaxation in the heterostructures under consideration are presented in **Table 1**. It is obvious that the distances are defined mainly by chalcogen atoms whereas metal atoms have a very small impact on the lattice. The stacking arrangement of the monolayers does not affect the distances between the atoms inside the layers.

Table 1. Distances (Å) between the metal atom (Me) and the chalcogen (X) atom in defect-free heterostructures, as well as between the impurity Te atom and the metal and chalcogen atoms.

	$MoS_2/MoSe_2$		MoS_2/WS_2		WS_2/WSe_2		$MoSe_2/WSe_2$	
	MoS_2	$MoSe_2$	MoS_2	WS_2	WS_2	WSe_2	$MoSe_2$	WSe_2
Defect-free structures								
Me-X	2.39	2.49	2.39	2.39	2.40	2.50	2.50	2.51
Structures with an impurity atom								
Te-Me	2.72	2.71	2.71	2.72	2.73	2.71	2.71	2.72
Te-X	3.29	3.27	3.23	3.23	3.29	3.27	3.33	3.33

© 2019 WILEY-VCH Verlag GmbH & Co. KGaA, Weinheim

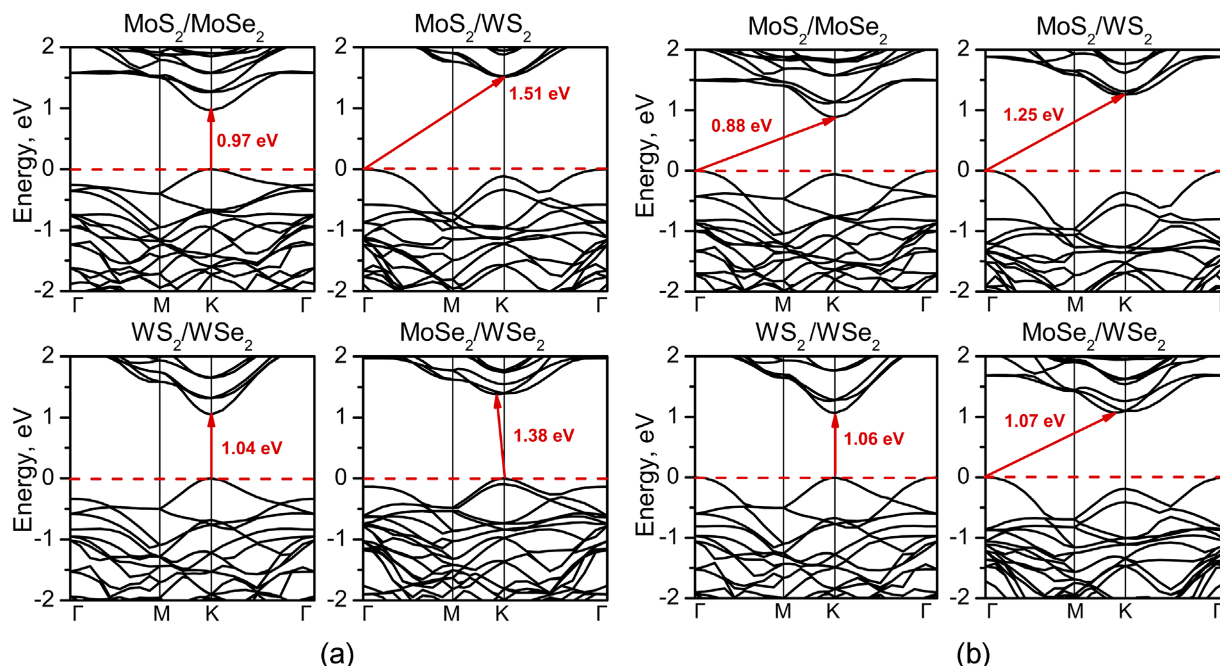

Figure 2. Electronic energy bands in $MoS_2/MoSe_2$, MoS_2/WS_2, WS_2/WSe_2, $MoSe_2/WSe_2$ heterostructures with the mirror arrangement of the monolayers (a) and with the monolayers shifted like in the bulk material (b). Zero on the energy scale corresponds to the Fermi level.

Substitution of S or Se atoms by Te ones increases the distance both to the nearest metal atom and to the nearest chalcogen one.

Figure 2a shows calculated electronic energy bands in the heterostructures composed of MoS_2, WS_2, WSe_2, and $MoSe_2$ monolayers with the mirror stacking arrangements. In case of combination of MoS_2 monolayer with $MoSe_2$ or WS_2 ones there is a direct electron transition through the gap of 0.97 eV in $MoS_2/MoSe_2$ heterostructure while an indirect transition of 1.51 eV between the Γ- and K-points is found in MoS_2/WS_2 heterostructure. In WSe_2 based couples WS_2/WSe_2 heterostructure has a direct transition of 1.04 eV at the K-point, while electronic bands in $MoSe_2/WSe_2$ heterostructure are characterized by an indirect transition of 1.38 eV since the conduction band minimum (CBM) is shifted from the K-point in the direction to the M-point.

The electronic energy bands calculated for the heterostructures with the shifted monolayers are presented in Figure 2b. These heterostructures retain semiconducting properties, however, indirect transitions become dominant. In $MoS_2/MoSe_2$ heterostructure the smallest energy gap is located between the Γ- and K-points and has the value of 0.88 eV. In WS_2/WSe_2 heterostructure there is a quasi-direct gap of 1.06 eV. In this case, the CBM is located at the K-point, while the valence band maxima (VBM) at the K- and the Γ-points have identical energy positions. MoS_2/WS_2 and $MoSe_2/WSe_2$ heterostructures have indirect gap of 1.25 and 1.07 eV, respectively, between the Γ-point and the point in the M-K direction. The mutual influence of the bands from individual layers could be traced through the dispersion of the bands.

Figure 3 illustrates total DOS for the two stacking arrangements of the defect-free monolayers and the monolayers with Te impurity in the site of chalcogen atoms. They are in general similar for all the structures considered, while there are some insignificant differences depending on the stacking arrangements of the layers.

Figure 4 presents a comparison of partial DOS in $MoS_2/MoSe_2$ heterostructures with the mirror and shifted arrangements of the monolayers. Their analysis showed: 1) the electronic states near the Fermi level are determined by *d*-electrons of the metal atoms with participation of *s*- and *p*-electrons of the chalcogen atoms; 2) the shift of the monolayers has no effect on the orbital composition; 3) the changes in spectrum dispersion are mostly quantitative.

In order to study an effect of point defects on the energy bands in the heterostructures, we put Te atom in the position of chalcogen one in each layer of $MoS_2/MoSe_2$, MoS_2/WS_2, WS_2/WSe_2, and $MoSe_2/WSe_2$ heterostructures (**Figure 5**a), as well modeled the case with a vacancy located in the position of the chalcogen atom in one layer, and the impurity atom in the other one (Figure 5b). Such configurations may refer to the case when each layer is fabricated and processed separately, that leads to different defects in each layer. Native defects like S vacancies in MoS_2 layers were already distinguished.[28] These vacancies behave very similarly both in a monolayer and in the bulk material slightly changing positions of surrounding atoms.[29]

The substitution of S or Se atoms by Te ones changes the character of the energy band gaps. The heterostructures become indirect-gap semiconductors with an exception of WS_2/WSe_2 possessing direct gap of 0.92 eV at the K-point. In $MoS_2/MoSe_2$ and MoS_2/WS_2 heterostructures, the transitions of 0.72 and 1.00 eV, respectively, occur between the Γ- and K-points, while in $MoSe_2/WSe_2$ the gap is increased to 1.10 eV and takes place between the Γ-point and the point lying in the M-K direction.

A comparison of the electronic energy band spectra in the defect-free (Figure 2) heterostructures and heterostructures doped by Te atoms (Figure 5) shows that the impurity atoms suppress the degeneracy and splitting of the energy levels in the

© 2019 WILEY-VCH Verlag GmbH & Co. KGaA, Weinheim

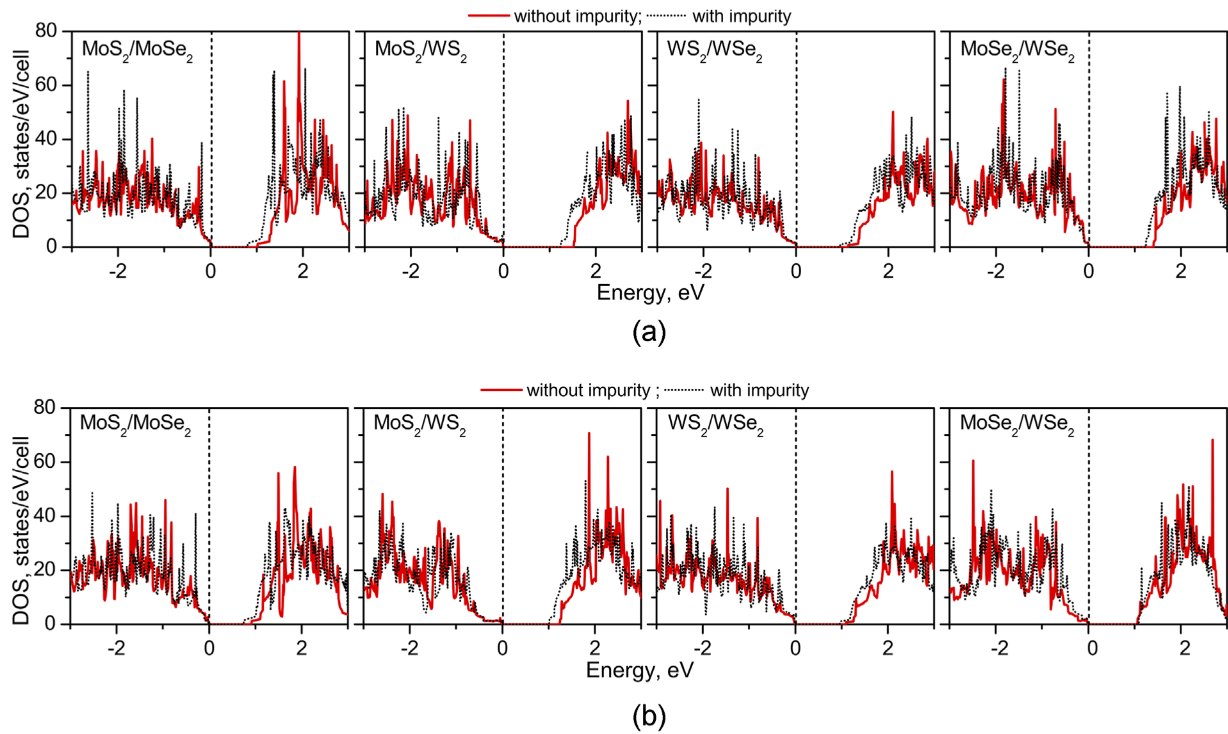

Figure 3. Total DOS in $MoS_2/MoSe_2$, MoS_2/WS_2, WS_2/WSe_2, $MoSe_2/WSe_2$ heterostructures with and without Te impurity in each monolayer: the heterostructures with the mirror arrangement of the monolayers (a) and with the monolayers shifted like in the bulk material (b). Zero on the energy scale corresponds to the Fermi level.

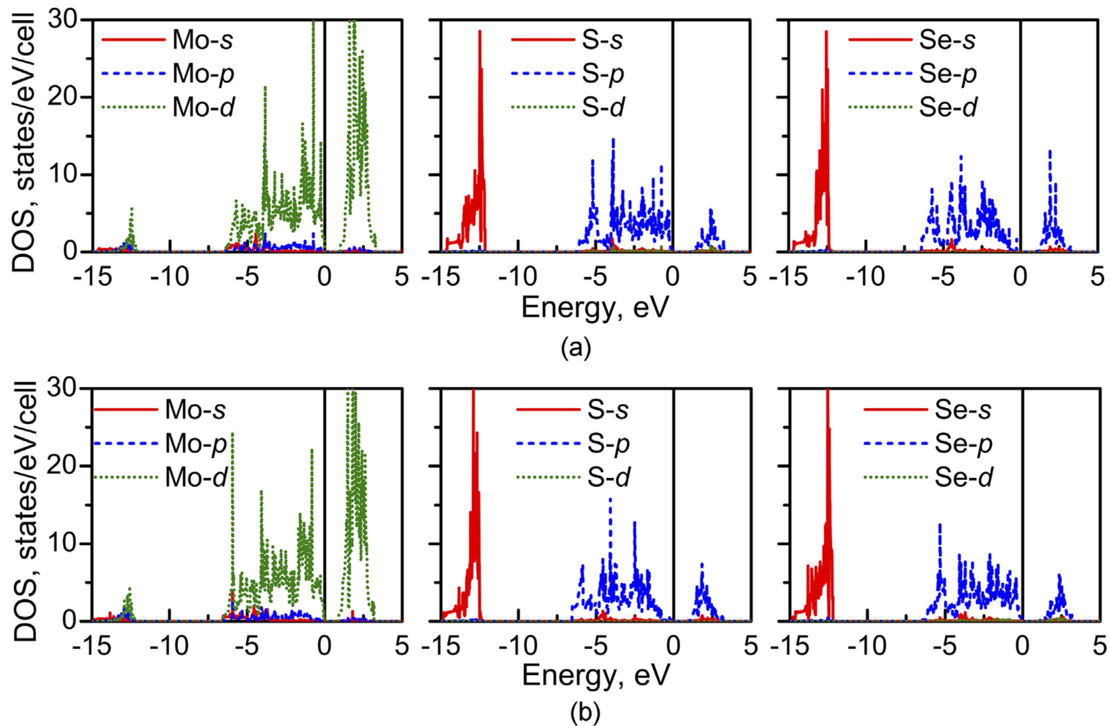

Figure 4. Partial DOS in $MoS_2/MoSe_2$ heterostructures with the mirror arrangement of the monolayers (a) and with the monolayers shifted like in the bulk material (b). Zero on the energy scale corresponds to the Fermi level.

© 2019 WILEY-VCH Verlag GmbH & Co. KGaA, Weinheim

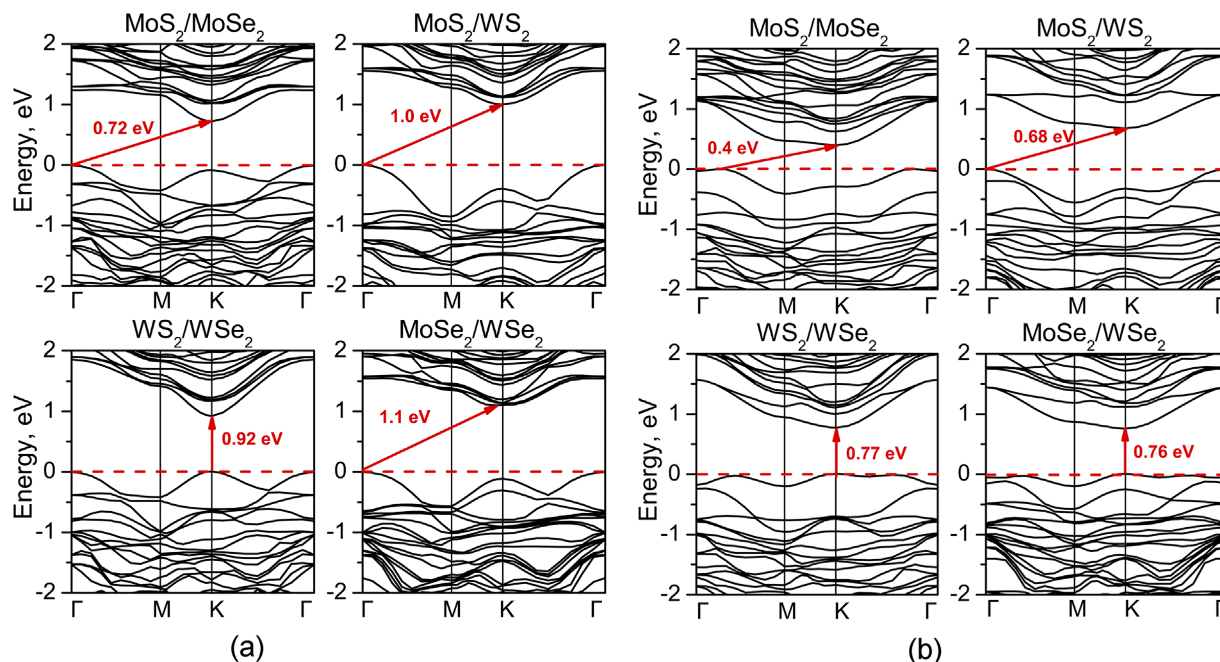

Figure 5. Electronic energy bands in $MoS_2/MoSe_2$, MoS_2/WS_2, WS_2/WSe_2, $MoSe_2/WSe_2$ heterostructures with Te atoms substituting the chalcogen atoms in each monolayer (a) and the impurity atoms and a vacancy in different monolayers (b) shifted like in the bulk material. Zero on the energy scale corresponds to the Fermi level.

conduction band, as well as shift the extrema and a decrease the band gap.

When both impurity atoms and vacancies are introduced (Figure 5b), the heterostructures behave in a special way: some of them exhibit a direct-gap character while the others remain indirect-gap semiconductors. So far, in $MoS_2/MoSe_2$ heterostructure the transition of 0.4 eV is indirect occurring between VBM at the Γ-K direction and CBM at the K-point. In MoS_2/WS_2 heterostructure there is an indirect transition of 0.68 eV between the Γ- and K-points. WS_2/WSe_2 and $MoSe_2/WSe_2$ structures have direct transitions at the K-point of 0.77 and 0.76 eV, respectively.

Significant changes in the electronic energy spectra in the heterostructures due to vacancies and substituting impurity atoms are evident. In the valence band, the dispersion of the bands varies significantly, and the band gap tends to decrease as compared to the defect-free structures. Energy levels in the band gaps are formed by unsaturated bonds of the atoms near vacancies.

Figure 6 presents total DOS in $MoS_2/MoSe_2$, MoS_2/WS_2, WS_2/WSe_2, $MoSe_2/WSe_2$ heterostructures with the shifted monolayers when both layers are doped by Te, as well as when there are Te atoms only in one of the layers while the other contains vacancies. New electronic states in the conduction band appeared in the heterostructures with both impurity atoms and vacancies if compared to the heterostructures containing only impurity atoms. The analysis of partial DOS (not presented) has shown that the electronic states near the Fermi level are mainly determined by *p*-electrons of the chalcogen atoms and *d*-electrons of the metal atoms located near vacancies.

The orbital compositions of the eigenstates at the main extrema points (Γ and K) have been analyzed in order to

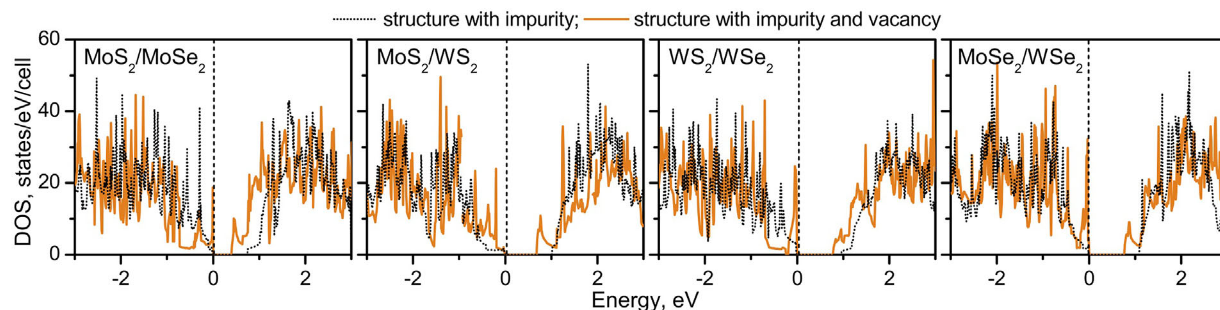

Figure 6. Total DOS in $MoS_2/MoSe_2$, MoS_2/WS_2, WS_2/WSe_2, $MoSe_2/WSe_2$ heterostructures with Te atoms substituting the chalcogen atoms in each monolayer, and with Te atoms substituting the chalcogen atoms and the impurity atoms and a vacancy in different monolayers shifted like in the bulk material. Zero on the energy scale corresponds to the Fermi level.

© 2019 WILEY-VCH Verlag GmbH & Co. KGaA, Weinheim

understand the above changes in the energy bands as well as for an estimation of the optical feasibility of the direct across-gap transitions. One should account for that electronic states forming VBM and CBM are highly delocalized. In some cases up to 50% of the charge is located in the interstitial region.

In spite of differences in the atomic composition and electronic energy band structures, one can trace some common regularities in the orbital compositions of the defect-free heterostructures studied. In the case of heterostructures with the mirror arrangements of the monolayers the upper valence band at the K-point is mainly composed by d_{xy} and $d_{x^2-y^2}$ orbitals of the metal (Mo or W) atoms (of about 30% each) with some small admixture of p_x and p_y orbitals of the chalcogen (S or Se) atoms (6% each). The upper valence band at the Γ-point includes d_{z^2} orbitals of the metal atoms (about 50%) with an admixture of p_z orbitals of the chalcogen (S or Se) atoms (of about 20%). There is a domination of d_{z^2} orbitals of the metal atoms (of about 75%) with a small admixture of some other orbitals in the lowest conduction band at the K-point. The shift of the monolayers does not change a lot the general orbital compositions at the high-symmetry points considered, while some quantitative variations are observed. There are no dramatic changes depending on the direct/indirect-gap character of the band structure.

The heterostructure WS_2/WSe_2 is found to be the most promising from a practical point of view. It has a direct gap independently on the arrangement of the monolayers; the orbital compositions at the K-point and electronic energy band structures are quite similar for both cases. The VBM is mainly characterized by d_{xy} and $d_{x^2-y^2}$ orbitals of W (28% each) with an admixture of p_x and p_y orbitals of Se (6% each). The CBM is formed mainly by the d_{z^2} orbitals of W (69%) combined with *s*-orbitals of W (6%).

The substitution of S(Se) atoms by Te ones does not radically affect the orbital composition.

In the other heterostructures with the shift of the monolayers the upper valence band at the K-point is still mainly characterized by d_{xy} and $d_{x^2-y^2}$ orbitals of the metal (Mo in case of $MoS_2/MoSe_2$ or W in other three cases) atoms (of about 30% each). The upper valence band at the Γ-point is composed by d_{z^2} orbitals of Mo or W atoms (of about 50%) with an admixture of p_z orbitals of the chalcogen (S or Se) atoms (of about 20%). The CBM at the K-point consists of d_{z^2} orbitals of Mo or W atoms (72 and 65%) in $MoS_2/MoSe_2$ and WS_2/WSe_2 heterostructures, respectively. Meanwhile, the heterostructures with different metals (MoS_2/WS_2 and $MoSe_2/WSe_2$) have more complex orbital compositions. In addition to d_{z^2} orbitals they include d_{xy} and $d_{x^2-y^2}$ orbitals of corresponding metals and even p_x and p_y (5% each) orbitals of Te in the doped $MoSe_2/WSe_2$ heterostructures. Vacancies in addition to Te atoms result in both VBM and CBM at the K-point to be composed of d_{xy}, $d_{x^2-y^2}$ (of about 20% each) and d_{z^2} (of about 10%) orbitals of Mo (in case of $MoS_2/MoSe_2$) or W (for three other heterostructures) atoms.

Hence, the analysis of the orbital compositions performed shows that the direct band gap (at the K-point) in the considered heterostructures with and without point defects is mainly formed by *d*-orbitals of the metal atoms at both VBM and CBM. Thus, optical transitions through this gap will be not allowed in the dipole approximation.

4. Conclusion

The performed computer simulation of electronic properties of the two-dimensional heterostructures formed by monolayers of MoS_2, WS_2, WSe_2, and $MoSe_2$ with different acceptable arrangements of the layers demonstrates them to have semiconductor properties different to those of individual monolayers. The heterostructures $MoS_2/MoSe_2$, MoS_2/WS_2, WS_2/WSe_2, and $MoSe_2/WSe_2$ with the monolayers shifted identically to the bulk materials behave like indirect-gap semiconductors, while their building monolayers are direct gap semiconductors. WS_2/WSe_2 and $MoS_2/MoSe_2$ heterostructures with mirror stacking of the monolayers retain the direct-gap character. Joint impact of vacancies and Te atoms substituting chalcogen atoms lead to a reduction of the energy gap and preservation of typical for the individual monolayers direct-gap character only in WS_2/WSe_2 and $MoSe_2/WSe_2$ heterostructures. The above peculiarities can be used for energy gap engineering in new electronic devices based on two-dimensional crystals.

Acknowledgements

This study has been partially supported by the Belarusian Republican Foundation for Fundamental Research (grant No: F17MC-017) and State Scientific Program "Functional and Engineering Materials, Nanomaterials". Financial support by the European Union within the MOST project is appreciated.

Conflict of Interest

The authors declare no conflict of interest.

Keywords

defects, electronic structure, heterostructures, transition metal dichalcogenides, two-dimensional crystals

Received: July 13, 2018
Revised: December 17, 2018
Published online:

[1] B. Radisavljevic, A. Radenovic, J. Brivio, V. Giacometti, V. A. Kis, *Nat. Nanotechnol.* **2011**, *6*, 147.
[2] B. Radisavljevic, M. B. Whitwick, A. Kis, *ACS Nano* **2011**, *5*, 9934.
[3] Z. Yin, H. Li, H. Li, L. Jiang, Y. Shi, Y. Sun, G. Lu, Q. Zhang, X. Chen, H. Zhang, *ACS Nano* **2012**, *6*, 74.
[4] Y. Zhang, J. Ye, Y. Matsuhashi, Y. Iwasa, *Nano Lett.* **2012**, *12*, 1136.
[5] H. Wang, L. Yu, Y.-H. Lee, Y. Shi, A. Hsu, M. L. Chin, L.-J. Li, M. Dubey, J. Kong, T. Palacios, *Nano Lett.* **2012**, *12*, 4674.
[6] I. Popov, G. Seifert, D. Tománek, *Phys. Rev. Lett.* **2012**, *108*, 156802.
[7] H. Qiu, L. Pan, Z. Yao, J. Li, Y. Shi, X. Wang, *Appl. Phys. Lett.* **2012**, *100*, 123104.
[8] K. S. Novoselov, D. Jiang, F. Schedin, T. J. Booth, V. V. Khotkevich, S. V. Morozov, A. K. Geim, *Proc. Natl. Acad. Sci. USA* **2005**, *102*, 10451.
[9] *Gmelin Handbook of Inorganic and Organometallic Chemistry*, 8th ed., Vol. B7, Springer-Verlag, Berlin **1995**. https://www.springer.com/series/562

© 2019 WILEY-VCH Verlag GmbH & Co. KGaA, Weinheim

[10] X. Su, W. Ju, R. Zhang, C. Guo, J. Zheng, Y. Yonga, X. Lia, *RSC Adv.* **2016**, *6*, 18319.
[11] K. F. Mak, Ch. Lee, J. Hone, J. Shan, T. F. Heinz, *Phys. Rev. Lett.* **2010**, *105*, 136805.
[12] H. Terrones, F. López-Urías, M. Terrones, *Sci. Rep.* **2013**, *3*, 1549.
[13] K. Kam, B. Parkinson, *J. Phys. Chem.* **1982**, *86*, 463.
[14] A. Splendiani, L. Sun, Y. Zhang, T. Li, J. Kim, C.-Y. Chim, G. Galli, F. Wang, *Nano Lett.* **2010**, *10*, 1271.
[15] F. Haque, T. Daeneke, K. Kalantar-zadeh, J. Z. Ou, *Nano-Micro Lett.* **2018**, *10*, 1.
[16] A. V. Krivosheeva, V. L. Shaposhnikov, V. E. Borisenko, J.-L. Lazzari, N. V. Skorodumova, B. K. Tay, *Int. J. Nanotechnol.* **2015**, *12*, 654.
[17] A. V. Krivosheeva, V. L. Shaposhnikov, V. E. Borisenko, J.-L. Lazzari, Ch. Waileong, J. Gusakova, B. K. Tay, *J. Semicond.* **2015**, *36*, 122002.
[18] E. Scalise, M. Houssa, G. Pourtois, V. Afanas'ev, A. Stesmans, *Nano Res.* **2012**, *5*, 43.
[19] H. P. Komsa, A. V. Krasheninnikov, *Phys. Rev. B* **2012**, *86*, 241201.
[20] J. Kang, S. Tongay, J. Zhou, J. Li, J. Wu, *Appl. Phys. Lett.* **2013**, *102*, 012111.
[21] D. Bocharov, S. Piskunov, Y. F. Zhukovskii, R. A. Evarestov, *Phys. Status Solidi RRL* **2019**, *13*, 1800253. https://doi.org/10.1002/pssr.201800253
[22] H. F. Liu, S. L. Wong, D. Z. Chi, *Chem. Vap. Deposition* **2015**, *21*, 241.
[23] D. M. Ceperley, B. J. Alder, *Phys. Rev. Lett.* **1980**, *45*, 566.
[24] G. Kresse, J. Furthmüller, *Phys. Rev. B* **1996**, *54*, 11169.
[25] R. Evarestov, A. Bandura, V. Porsev, A. Kovalenko, *J. Comput. Chem.* **2017**, *38*, 2581.
[26] J. Klimeš, D. R. Bowler, A. Michaelides, *Phys. Rev. B* **2011**, *83*, 195131.
[27] A. V. Krivosheeva, V. L. Shaposhnikov, V. E. Borisenko, *Vestnik Found. Fundamental Res.* **2016**, *77*, 41 (in Russian).
[28] H.-P. Komsa, A. V. Krasheninnikov, *Phys. Rev. B* **2015**, *91*, 125304.
[29] J.-Y. Noh, H. Kim, Y.-S. Kim, *Phys. Rev. B* **2014**, *89*, 205417.

© 2019 WILEY-VCH Verlag GmbH & Co. KGaA, Weinheim